IEEE Access
Multidisciplinary | Rapid Review | Open Access Journal

Received 12 February 2024, accepted 3 March 2024, date of publication 11 March 2024, date of current version 3 April 2024.

Digital Object Identifier 10.1109/ACCESS.2024.3376513

RESEARCH ARTICLE

Analysis and Modeling of Direct Ammonia Fuel Cells for Solar and Wind Power Leveling in Smart Grid Applications

MISWAR A. SYED[1], (Member, IEEE), OSAMAH SIDDIQUI[2], (Member, IEEE), MEHRDAD KAZERANI[1], (Life Senior Member, IEEE), AND MUHAMMAD KHALID[3,4], (Senior Member, IEEE)

[1]Department of Electrical and Computer Engineering, University of Waterloo, Waterloo, ON N2L 3G1, Canada
[2]School of Engineering, The University of British Columbia, Kelowna, BC V1V 1V7, Canada
[3]Electrical Engineering Department, King Fahd University of Petroleum and Minerals (KFUPM), Dhahran 31261, Saudi Arabia
[4]Interdisciplinary Research Center for Sustainable Energy Systems, King Fahd University of Petroleum and Minerals (KFUPM), Dhahran 31261, Saudi Arabia

Corresponding author: Miswar A. Syed (miswar.syed@uwaterloo.ca)

This work was supported by the Natural Sciences and Engineering Research Council of Canada (NSERC).

ABSTRACT Integration of wind and solar energy sources in power systems causes frequency and voltage-related power quality issues, especially at high penetration levels. Battery energy storage systems help reduce fluctuations by absorbing excess power and delivering power deficits. However, batteries suffer from capacity fading and degradation due to frequent cycling. Storing energy in the form of a chemical fuel helps in overcoming these drawbacks. Since ammonia fuel cells address issues associated with hydrogen fuel cells, such as high flammability, poor volumetric density, and high storage costs, in this study the application of ammonia fuel cells for solar and wind power leveling is investigated. Excess wind/solar power is used in an electrochemical ammonia synthesizer (EAS) to produce ammonia, and a direct ammonia fuel cell (DAFC) converts the ammonia to electric power and supplies the power deficit. Smoothing filter concepts, such as moving average, moving median, Savitzky-Golay, moving regression (MR), and Gaussian filters, are employed to assess EAS and DAFC capacity requirements. Simulation results show that MR filter's overall performance is superior to those of other smoothing filter approaches, resulting in reduced required capacities for ammonia production and fuel cell output, lowering system costs. The developed energy storage system is an effective compensation method for solar and wind power fluctuations.

INDEX TERMS Fuel cells, power smoothing, smoothing filters, wind power, solar power, green hydrogen, green ammonia synthesis.

NOMENCLATURE

V_{ac-EAS}	Activation polarization voltage overpotential.
$V_{cnc-EAS-an}$	Voltage overpotential due to concentration polarization at the anode.
$V_{cnc-EAS-ct}$	Concentration polarization overpotential.
β	Array of linear parameters.
β^T	Transpose of the matrix X.
ΔG^0	Standard Gibbs energy change.
δ_{an}	Electrode thickness at the anode.
δ_{ct}	Electrode thickness at the cathode.
$\dot{P}_{EAS-in}$	Electrochemical ammonia synthesizer power input requirement.
σ	Gaussian filter standard deviation.
a	Height of the Gaussian curve's maximum.
A_{DAFC}	Total electrode area of direct ammonia fuel cell.
b	Gaussian peak's position in the middle.
c	Breadth of the Gaussian root mean square.
$D^e_{N_2}$	Effective coefficient of diffusion for nitrogen gas.

The associate editor coordinating the review of this manuscript and approving it for publication was Padmanabh Thakur.

F	Faraday's constant.
f	Frequency.
f_c	Corner frequency of the moving average filter.
$h(n)$	Savitsky Golay filter's impulse response.
I_{0-EAS}	Exchange current density.
$I_{tot-EAS}$	Electrochemical ammonia synthesizer total current input.
k	Neighboring data points of the target value.
M	Savitsky Golay filter smoothing parameter.
N	Number of data points in the solar and wind power profile.
n	Electron count.
P	Gaseous pressure.
P_{fluc}	Fluctuating solar and wind power.
$P^0_{N_2}$	Nitrogen gas partial pressure.
P_{ref}	Power output of the smoothing filters.
R	Gas constant.
T_f	Low pass filter time constant.
T_S	Control period.
T_{MA}	Period of the moving average filter.
$V_{ac-DAFC}$	Activation polarization induced voltage loss.
$V_{cnc-DAFC}$	Voltage loss due to concentration polarization.
$V_{OC-DAFC}$	Open circuit voltage of direct ammonia fuel cell.
V_{OC-EAS}	Open circuit voltage of the electrochemical ammonia synthesizer.
$V_{Ohm-DAFC}$	Ohmic loss in voltage.
$V_{OPN-DAFC}$	Operational voltage of direct ammonia fuel cell.
$V_{OPN-EAS}$	Overall cell voltage.
W	Matrix containing all the determined weights.
$w(x)$	Distance weights.
x	Target data point.
x'	Distance from the target data point.
$x(n)$	Input vector of fluctuating data points.
$Y(n)$	Median value of the input vector.
$\dot{N}_{DAFC-NH_3}$	Molar consumption rate of ammonia.
I_{D-DAFC}	Operational current density of direct ammonia fuel cell.
I_{D-EAS}	Actual current density.
T_{EAS}	Operational temperature of the electrochemical ammonia synthesizer.

I. INTRODUCTION

Excessive use of fossil fuels in the past decades has increased the level of greenhouse gases in the atmosphere, with serious adverse environmental consequences [1]. Globally, various initiatives are being taken to lessen reliance on fossil fuels and increase the use of environmentally-friendly renewable sources of energy, such as solar, wind, and hydro [2]. Unfortunately, the intermittent and fluctuating nature of these energy sources can result in rapid variations in the voltage and frequency at high penetration levels, introducing challenges to stable operation of the grid [3]. Thus, renewable energy sources are integrated within a grid through microgrids, and energy storage technologies are employed to regulate and stabilize wind and solar power outputs (as shown in Fig. 1) [2], [4]. The excess power that is available during periods of intense solar irradiation or wind speeds can be stored, and the stored energy can be used, as required, during times of low wind speed or solar irradiation [3]. The need for energy storage has strengthened the search for appropriate energy storage techniques. Batteries and thermal energy storage are currently the most prevalent storage methods. Yet, these systems are accompanied by their own unique geographical, technological, environmental, and economic constraints [5], necessitating the development of novel energy storage techniques and technologies.

In order to deal with the unpredictable nature of wind power, several energy storage systems (ESSs) are being used in the electricity generation industry, including batteries, supercapacitors, flywheels, and fuel cells (FCs) [6]. Even though batteries are the most common medium for energy storage, FCs have several advantages that can alleviate the difficulties currently faced by batteries [5]. In particular, FCs operate based on a chemical fuel, circumventing the issue of energy storage capacity fading in batteries. Since, in FCs, energy is retained in chemical form, storage durations can be extended significantly without any loss of energy quantity or quality, unlike with batteries. Moreover, increased storage capacity flexibility is achieved by the introduction of chemical fuels for energy storage [7], [8].

The most popular energy storage technology used in wind power systems is battery storage [9]. The traditional storage technology for solar thermal power plants, like solar towers, is thermal energy storage [10]. The drawbacks of such energy storage techniques include issues with sizing and lifespan, high cost, and negative impact on the environment. When excess power is available, it can be used to produce a green fuel like hydrogen or ammonia. Then, these fuels can be used to produce electricity when there is a shortage of energy. The fuel that is believed to displace fossil fuels in the coming years is hydrogen. But extensive use of hydrogen has been hindered due to its high flammability and low volumetric density [10], [11]. Recently, ammonia has been recognized as a viable hydrogen-containing alternative, capable of providing clean and environmentally friendly energy. There are various benefits to storing hydrogen chemically in the form of ammonia, including reduced storage and transportation complications, larger volumetric density, more hydrogen atoms per ammonia molecule than hydrogen molecule, and decreased flammability [12]. Ammonia synthesis using wind power was investigated in [13] for remote islands. Hydrogen was produced using alkaline water electrolysis, and desalination was carried out using vapor compression. The Haber-Bosch process method served as the foundation for the ammonia production process. Authors in [14] investigated a

thermochemical ammonia storage approach that made use of and stored solar thermal energy. Solar energy was used to split ammonia into its components, i.e., hydrogen and nitrogen, whereas the energy produced during the ammonia synthesis process was used as the system output. The study discovered that due to their greater heat transmission capacities, reactors with smaller diameters are preferred for such systems. Reference [15] examined an ESS based on ammonia and strontium chloride. To store the energy, the plant made use of ammonium-strontium chloride thermochemical interactions. The proposed system's energetic and exergetic efficiencies during heat generation at temperature of 87°C was found to be 65.4% and 50.8%, respectively. Also, it was determined that the peak heat and cold energies produced were 2010 and 902 kJ/kg, respectively. Ammonia was studied in [16] due to its potential as a fuel for ships and as a means of storing energy. The effectiveness of the system under consideration was compared to that of various energy storage methods, including batteries and hydrogen fuel. It was concluded that the infrastructure for ammonia-based energy storage is a viable choice. A combined solar and wind-based system was proposed in [17] to manufacture ammonia and electrical power. The necessary hydrogen gas was generated using a water electrolysis process based on a proton exchange membrane (PEM). Furthermore, ammonia was created using a multistage synthesis technique. The system's maximum energy efficiency was determined to be 75.8%, while its stated exergetic efficiency was 73.6%. Ammonia was taken into consideration as a form of energy storage for solar farms in [18]. Units for the manufacture of hydrogen, nitrogen, and ammonia utilized the additional power available. It was concluded that the synthesis phase accounted for more than 90% of the overall cost in the designed system. The work in [19] considered 1 to 10 MW islanded ammonia energy systems. The research studied the synthesis of hydrogen and nitrogen through PEM water electrolysis and pressure swing adsorption, respectively. It was discovered that the overall round-trip efficiency of the islanded system was 61%. Using the enhanced process integration method, [20] looked at an ammonia-based power generation system. The technique combines process integration and exergy recovery. These techniques were intended to reduce the energy loss of the entire process. Moreover, for storage, ammonia was created from the hydrogen produced. The designed system's total efficiency was determined to be 66.9%. Researchers in [21] investigated the power-to-ammonia pathway, and an ammonia-based system with 100% renewable penetration was presented. An ESS using ammonia in a multigenerational system was thermodynamically evaluated in [22] and [23]. According to the stated efficiencies, the system's exergetic efficacy was 18% and its energetic performance was 28%. The ammonia created was used as fuel for vehicles and as fertilizers in agriculture.

The employment of hydrogen fuel cells for energy storage has been examined in prior studies. A dynamical system model was constructed to analyze the performance of the

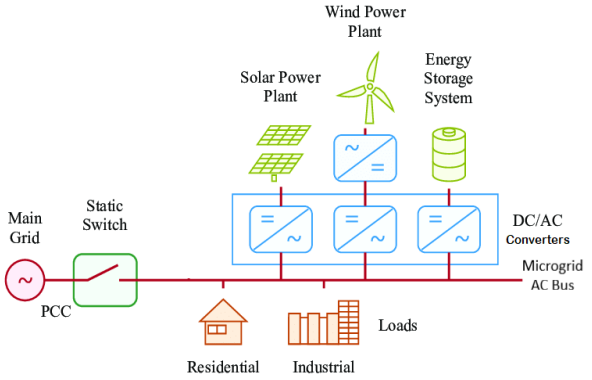

FIGURE 1. A microgrid with renewable sources and energy storage [2].

system. In [24], a wind power leveling system via hydrogen FCs was simulated. The steady load tracking was examined via optimal control design and successive iterations. The tuning was aimed at saving system components and lowering operating costs. With intermittent renewable energy systems, hybrid battery and FC devices have also been presented [25]. The electrochemical hybrid ESS was found to have the ability to take the place of diesel generators for regulating the output of wind and solar energy systems. A hybrid wind-solar-based stand-alone energy system using an Electrolyzer-FC technology was assessed [26]. This system generated hydrogen when there was an excess of solar and wind energy outputs and used the hydrogen that had been stored when there was a shortage of solar and wind energy. Additionally, research was done to plan the use of hydrogen-based ESS for wind turbines [27], [28]. ESS powered by fuel cells has been created to address the power quality issues brought on by unpredictable wind power outputs [29]. Considering the numerous technological constraints associated with wind turbines, these technologies were developed for hybrid renewable energy systems. Direct ammonia fuel cells (DAFC) have not yet been thoroughly studied for power smoothing applications, the usage of hydrogen fuel cells (FC) to smooth the output of wind turbines was studied in earlier studies. However, there are a number of problems with hydrogen, including low volumetric density, high flammability, and expensive storage costs, all of which could be reduced by using DAFC. Ammonia can help to eliminate the current problems with hydrogen by requiring a far lower storage cost as well as an increase in volumetric capacity [30], [31].

As established above, DAFC has a variety of advantages over hydrogen FC. Yet, its potential for regulating and smoothing the fluctuating solar and wind power remains to be examined. Also, it is crucial to research the application of various smoothing filters and their effect on the DAFC and EAS systems. Furthermore, it's important to assess the necessary EAS and DAFC capacities linked to the application of various power smoothing filters, as lower capacities directly reduce the overall system costs. Currently, smoothing filters are employed in combination with BESS to minimize the battery charging and discharging power,

which further lowers the system cost [32]. To smooth the output power, several smoothing filters have previously been developed and integrated with BESSs. The most widely used filtering methods are Low Pass (LP), Moving Average (MA), Moving Median (MM), Gaussian (G), Savitsky Golay (SG), and Moving Regression (MR) filters. Reference [33] has reported that the use of low pass filters prior to injecting fluctuating power into the grid causes a severe lag in the resulting output power. Thus, the battery's capacity for both charging and discharging is greatly increased. It was reported in [34] that the MA filter had much better flattening and power-following characteristics than the LPF. Longer LPF time constants and larger MA filter window sizes increase smoothness, however, they do so at the expense of a time delay, necessitating the use of larger batteries [33]. A longer LPF time constant has a negative effect on battery charging and discharging power, according to the authors of [35]. The battery's SoC is frequently changed by insufficient power tracking, which increases the number of cycles the battery experiences and reduces its lifespan [36]. An MM filter was created and compared to LPF and MA filters in [33]. The findings indicated that while the MM filter offers greater power tracking at the expense of less effective solar power smoothing, it does so with window widths similar to those of an MA filter. A G filter is recommended in [34] and [37] to smooth a wind turbine's output power. A GF tends to over-smooth the power, which results in the loss of power signal characteristics, as was discovered in [38]. This causes a deep discharge of the battery, which reduces battery life [39]. In order to reduce solar PV variability, power lagging, and battery charging/discharging power, an MR filter has been proposed in conjunction with SoC feedback management [34]. The findings show that an MR filter enhances solar power flatness while maintaining BESS capacity. Finally, the SG filter combined with a control mechanism overcomes the difficulty of power tracking and generates a level of smoothness compared to the MA filter while reducing storage capacity [35].

This paper proposes and demonstrates the use of DAFC for power smoothing applications based on controlled electrochemical ammonia synthesis. The excess solar and wind power available is supplied to the EAS for ammonia production through which the energy can be stored for extended periods of time. Several power-smoothing filters, such as MA, MM, MR, SG, and GF have been employed to provide the required power reference for the EAS. Based on the filter output, if the solar/wind power exceeds the required smoothed power output, it is utilized to synthesize ammonia using the EAS; otherwise, if the solar/wind power falls short of the required smoothed output, the DAFC can be utilized to supply the deficit power. A comparative study of the filters is conducted with different window sizes to investigate the degree of smoothness and power tracking capabilities. The EAS and DAFC capacity requirements are determined and tied to the system's economic performance. Larger capacity requirements necessitate higher capital and operational expenditures. Simulation results have concluded that MR filter has a superior overall performance as it has excellent power tracking and smoothing capabilities, while resulting in lower ammonia production capacity and lower fuel cell output capacity, thereby reducing the overall system cost. The proposed approach contributes to knowledge and technology by introducing a new application for DAFC as a means for solar/wind power smoothing through filter-based controlled ammonia production and storage.

The remainder of the paper is organized as follows. Section II provides the problem statement. Section III describes the proposed methodology and modeling of the MA, MM, MR, SG, and Gaussian filters, as well as the EAS and DAFC. Section IV introduces the datasets used in this study. Section V examines the simulation results and draws crucial conclusions concerning the system performance. Finally, section VI concludes the paper and provides recommendations for future research.

II. THE PROBLEM FORMULATION

The present research addresses the output power fluctuations of renewable energy sources. Power smoothing filters are implemented to extract the signal representing the power that can be used to produce smooth power via EAS and DAFC. Even though electrolyzers and hydrogen FCs can serve the same purpose, the higher cost of storage of hydrogen [18] and substantially larger volumetric density, and lower safety risk of ammonia put ammonia in a superior position with respect to hydrogen. This is a motivation for research on the use of ammonia in the context of an energy storage system for smoothing variable power outputs of intermittent sources of energy. Several filter-based control systems have been previously proposed to smooth out solar and wind power fluctuations. Some common filtering techniques can provide the required reference for the smooth output power; however, this comes at the expense of a large time delay, which increases the capacity requirements of storage systems and cost of the overall system, as a result. This calls for a comparative study to identify a filter that provides reasonably smooth output with reduced time delays.

The objectives of the research reported here are: (i) to introduce, design, and implement a power control strategy based on the utilization of ammonia as a form of ESS, employing the EAS and DAFC, for integration of solar and wind energy; (ii) to analyze the capacity requirements of the EAS and DAFC through the application of several power smoothing filters such as the MA, MM, MR, SG, and GF; and (iii) to conduct a comparison among various filters based on window sizes, to study the power lagging phenomenon and its effect on the EAS and DAFC capacity requirements.

III. THE PROPOSED METHODOLOGY AND MODELING

The proposed scheme for smoothing the fluctuating power output of solar and wind energy systems via electrochemical ammonia synthesis and direct ammonia fuel cells is demonstrated in Fig. 2. The fluctuating power output of renewable

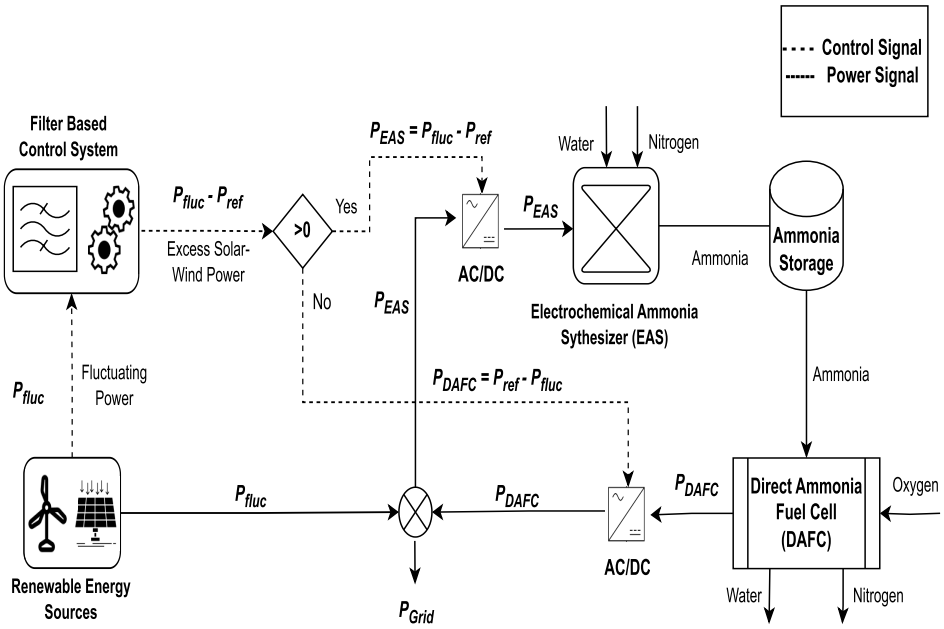

FIGURE 2. The Proposed solar and wind power control strategy via electrochemical ammonia synthesis and direct ammonia fuel cells utilization.

energy source, P_{fluc}, is first passed through the filter-based control system to get the excess power available for the EAS. The MA, MM, MR, SG, and GF smoothing filters considered in this research are popular methodologies and have previously been proposed in combination with BESS for control system design and power firming [34]. The output of the smoothing filters P_{ref} is subtracted from P_{fluc} to determine the excess solar and wind power available that can be supplied to the EAS. When $P_{fluc} > P_{ref}$, the excess power available, P_{EAS}, is provided as input to the EAS subsystem; power is supplied to EAS to generate ammonia. On the contrary, when $P_{fluc} < P_{ref}$, DAFC uses stored ammonia to produce electric power P_{DAFC}. P_{Grid} denotes the overall smoothed power supplied to the grid. The mathematical modelling of different system components is described in the following subsections.

A. MOVING AVERAGE (MA) FILTER

Moving average filtering is a power-firming technique that computes on-the-fly averages to smooth out oscillations in the time series of intermittent power data using a sliding window. The real solar/wind power data and the MA filter's window size are the required inputs to the algorithm. The power available for the electrochemical ammonia synthesizer depends on the difference between the power output of the MA smoothing algorithm (P_{ref}) and the actual variable power data (P_{fluc}) [40]. Although using larger window widths results in a smoother output, they cause power lagging, resulting in increased charging and discharging power of the integrated battery, thereby increasing the battery capacity requirement and the associated costs [36], [41]. The smoothed output power using the MA filter is obtained using [40]:

$$P(t) = \frac{1}{N} \sum_{i=0}^{N-1} P_{Wsys}\,(t - i \cdot T_S) \tag{1}$$

The number of data points, N in (1), is computed as $N = T_{MA}/T_S$, where T_{MA} denotes the moving average filter's period and T_S denotes the control period. The characteristic gain of MA filter is given by (2), where f is the frequency [36].

$$G_{MA}(f) = \frac{T_S}{T_{MA}} \cdot \frac{\sin(\pi \cdot f \cdot T_{MA})}{\sin(\pi \cdot f \cdot T_S)} \tag{2}$$

The characteristic phase of the MA filter is expressed as follows [42]:

$$\phi_{MA}(f) = \tan^{-1}\left\{\frac{X_{MA}}{Y_{MA}}\right\} \tag{3}$$

where,

$$\begin{aligned} X_{MA} = {} & \sin(2\pi f \cdot T_{MA})(1 - \cos(2\pi f \cdot T_S)) \\ & - \sin(\pi f \cdot T_S)(1 - \cos(2\pi f \cdot T_{MA})) \end{aligned} \tag{4}$$

and

$$\begin{aligned} Y_{MA} = {} & \sin(2\pi f \cdot T_{MA})(\sin(2\pi f \cdot T_S) \\ & + (1 - \cos(2\pi f \cdot T_{MA}))(1 - \cos(2\pi f \cdot T_S)) \end{aligned} \tag{5}$$

Finally, the corner frequency of the MA filter is computed as [43]:

$$f_c = \frac{\sqrt{2}}{\pi \cdot T_{MA}} \tag{6}$$

B. MOVING MEDIAN (MM) FILTER

Like the MA filter, MM filter uses a window with a defined length for smoothing. However, the MM filter determines the median of a vector whose length is determined by the window size rather than averaging across the window. When there are more outliers in the enclosed data, the moving median filter is very effective. In other words, an MM filter will handle the data more effectively than the MA filter if the input fluctuating power data inside the chosen window includes an abundance of outlying data points. When there are insufficient data points for the entire window, the window will automatically shrink in size. MM filter is used in the study in [44] to smooth solar output power, and its performance is compared to that of MA filter. The sliding window across the median value $y(n)$ of neighbouring values is obtained as follows [42]:

$$Y(n) = f(x(n)), x(n-1), \ldots x(n-m), (n-1), \\ y(n-2), \ldots y(n-m) \tag{7}$$

where

$$x(n) = [x(n), x(n-1), \ldots x(n-m)]^T \tag{8}$$

The output $Y(n)$ indicates the median value for the specified $x(n)$ input vector of fluctuating data points.

$$y(n) = med\{x(i)\}, \quad i = n, n-1, n-m \tag{9}$$

Whenever an odd window size is specified, the window surrounds the element in its present location. In contrast, if the window size is even, the prior and current data points are surrounded by the window.

C. MOVING REGRESSION (MR) FILTER

The MR filter is a non-parametric smoothing filter that eliminates the variations at each time step by using the linear regression ML principle [34]. The MR filter uses the window size as the input operational variable, just as the MA and MM filters. The training data for the linear regression technique are the k nearby data points of the target value. As a result, the window size of the MR filter affects how many nearby data points are employed to train the linear regression model. The more data used for training, the larger the window size, and the more accurate the estimated smoothed value will be [36]. Priority weights are given to the nearby data points depending on how far they are from the target value. As the distance from the target value grows, the weight assigned to that individual data point is reduced. The Tricubic function is employed to calculate the distance weights $w(x)$ for every k neighbors of x based on the distance x':

$$w(x) = \begin{cases} (1-|x|^3)^3, & |x| < 1 \\ 0, & |x| \geq 1 \end{cases} \tag{10}$$

Normalizing (10) so that larger distances are associated with lower weights:

$$w(x) = \begin{cases} (1-|\frac{d(x,x')}{max_i d(x_i,x')}|^3)^3, & |x| < 1, x_i \in D \\ 0, & |x| \geq 1 \end{cases} \tag{11}$$

where the distance between the closest neighbours k and x' is $d(x, x')$. Locality is accomplished by giving the data point nearest to x' the utmost priority and the data point farthest from x' the least priority. As a result, points that are farthest away from x' will have zero value for the weight, while the data point that is closest to x' will have a weight of 1, i.e., the maximum weight. The regression model of the MR employs the collected values of x and y as entries to the linear regression algorithm to compute the output estimate y' using the normalised first-degree linear regression technique [36].

$$\beta = (X^T W X)^{-1} X^T W Y \tag{12}$$

where W is the matrix containing all the determined weights, X and Y are the arrays storing all x and y values, accordingly, and β is the array of linear parameters. The updated values of y for firmed solar or wind power output generation are determined using (13), where β^T denotes the transpose of the matrix X.

$$y' = \beta^T X \tag{13}$$

D. GAUSSIAN (G) FILTER

Gaussian filter has an impulse response that approximates the Gaussian function presented in (14). A G filter has the lowest possible group delay and no overshooting characteristics while reducing rise and fall times. The variable power produced by renewable energy sources is flattened by the G filter smoothing [45]. Comparable to the MA filter, a G filter utilizes a moving window; however, the extent of smoothness is governed by the standard deviation of the Gaussian rather than the averaging method, making the outcome of the Gaussian filter a bell-shaped distribution [34].

$$f(x) = a.\exp(\frac{-(x-b)^2}{2c^2}) \tag{14}$$

In (14), a is the height of the curve's maximum, b is the peak's position in the middle, and c represents the standard deviation or the breadth of the Gaussian root mean square. The GF can be implemented as follows in one dimension [45]:

$$G(x,\sigma) = \frac{1}{\sqrt{2\pi}} \exp(\frac{-x^2}{2\sigma^2}) \tag{15}$$

The Gaussian filter standard deviation is represented by σ.

E. SAVITSKY-GOLAY (SG) FILTER

A Savitsky-Golay filter employs the method of least square of polynomial approximation across a sliding window. As a result, SG filter is often referred to as a least squares polynomial filter. By using an unweighted linear least square fit with a polynomial of a specific degree, the filter

coefficients are determined. A significant benefit of the SG filter over the MA filter is its ability to retain important data characteristics like amplitude, breadth, and peaks of the input signal, which are typically lost when using the MA filter. As the polynomial order of the filter is increased, the SG filter's performance tends to improve [40]. An SG filter, however, is only limited to odd numbers for the window sizes, and it is less efficient at eliminating noise than the MA filter. Using an SG filter on a given batch of fluctuating data of the form:

$$y(n) = x(n) + w(n) \tag{16}$$

where $x(n)$ denotes the time series data, and the noise in $y(n)$ is given by $w(n)$. The SG filter output power $\hat{x}(n)$ is computed as follows:

$$\hat{x}(n) = \sum_{k=-M}^{M} h(n)y(n-k) \tag{17}$$

Here, M stands for the SG filter smoothing parameter and $h(n)$ represents the filter's impulse response across $(|n| \leq M)$. At $(n = 0)$, $\hat{x}(n)$ is defined as the coefficient of the polynomial of order k that best fits $y(n)$ across $(|n| \leq M)$. The symmetric feature of the impulse response at $(n = 0)$ should allow for the fulfillment of the condition $(0 < k \leq 2M)$ for the polynomial order of k [33]. The squared error formula defined in (18) is used to determine the difference between the smoothed and unsmoothed signals, with $p(n)$ represented by the polynomial in (19).

$$E = \sum_{n=-M}^{M} (y(n) - p(n))^2 \tag{18}$$

$$p(n) = \sum_{k=0} C_k n^k \tag{19}$$

The following relationship exists between the impulse response $h(n)$ and the SG filter's transfer function [42]:

$$H(z) = \sum_{n} h(n) z^{-n} \tag{20}$$

F. ELECTROCHEMICAL AMMONIA SYNTHESIZER (EAS)

In the present study, an electrochemical ammonia synthesis (EAS) system is employed for utilizing the surplus power signals available during the process of smoothing solar or wind power outputs. The overall reaction that represents the synthesis of ammonia in the EAS is as follows [18]:

$$N_2 + 3H_2O \leftrightarrow 2NH_3 + \frac{3}{2}O_2 \tag{21}$$

First, the voltage of the EAS is determined under open circuit conditions (V_{OC-EAS}) according to [10]:

$$V_{OC-EAS} = \frac{-\Delta G^0}{nF} + \frac{T_{EAS}R}{nF} \ln\left(\frac{P_{NH_3}}{P_{N_2}^{0.5} P^{1.5}{}_{H_2}}\right) \tag{22}$$

where the standard Gibbs energy change is written as ΔG^0, the operational temperature is denoted by T_{EAS}, the gaseous pressure is represented by P, the gas constant is written as R, the Faraday's constant is represented by F, and the participating electron count is n.

Further, the actual operational voltage of the EAS depends on the extent of ohmic, activation, and concentration polarization voltage overpotentials. The overall cell voltage during operation can thus be written as [10]:

$$V_{OPN-EAS} = V_{OC-EAS} + V_{ac-EAS} + V_{cnc-EAS} + V_{Ohm-EAS} \tag{23}$$

where the activation polarization voltage overpotential V_{ac-EAS} is calculated from the exchange current density (I_{0-EAS}), actual current density during operation (I_{D-EAS}), and operational temperature (T_{EAS}) as [10]:

$$V_{ac-EAS} = \ln\left(\frac{I_{D-EAS}}{2I_{0-EAS}}\right)\frac{T_{EAS}R}{Fn} \tag{24}$$

Also, the concentration polarization overpotential of voltage can be evaluated as:

$$V_{cnc-EAS-ct} = \ln\left(1 + \frac{I_{D-EAS}T_{EAS}R\delta_{ct}}{nFP_{N_2}^0 D_{N_2}^e}\right)^{\frac{1}{2}} \frac{RT_{EAS}}{nF} \tag{25}$$

where δ_{ct} denotes the electrode thickness at the cathode, $D_{N_2}^e$ represents the effective coefficient of diffusion for nitrogen gas, and $P_{N_2}^0$ is the nitrogen gas partial pressure. Moreover, the voltage overpotential due to concentration polarization at the anode is determined as follows [10]:

$$V_{cnc-EAS-an} = \ln\left(\frac{1 + \frac{\delta_{an}I_{D-EAS}T_{EAS}R}{nFD_{NH_3}^e P_{H_2}^0}}{1 - \frac{\delta_{an}I_{D-EAS}T_{EAS}R}{nFD_{NH_3}^e P_{NH_3}^0}}\right)\frac{RT_{EAS}}{nF} \tag{26}$$

where the electrode thickness at the anode is represented as δ_{an}. The power input requirement of the EAS subsystem at a given operational point is evaluated from the operational voltage and total current input $(I_{tot-EAS})$ as [18]:

$$\dot{P}_{EAS-in} = V_{OPN} I_{tot-EAS} \tag{27}$$

G. DIRECT AMMONIA FUEL CELL (DAFC)

DAFC is utilized in the present study to mitigate the power deficits during power smoothing. Ammonia reacts electrochemically in the DAFC according to the following overall reaction [10]:

$$2NH_3 + \frac{3}{2}O_2 \rightarrow N_2 + 3H_2O \tag{28}$$

where the operational current of the DAFC is related to the ammonia consumption rate according to [18]:

$$\dot{N}_{DAFC-NH_3} = \frac{I_{D-DAFC}A_{DAFC}}{nF} \tag{29}$$

where $\dot{N}_{DAFC-NH_3}$ represents the molar consumption rate of ammonia in the DAFC, I_{D-DAFC} denotes the operational current density of the DAFC, and A_{DAFC} is the total electrode area of the DAFC.

The operational DAFC voltage is evaluated as a function of the DAFC open circuit voltage ($V_{OC-DAFC}$), activation polarization induced voltage loss ($V_{ac-DAFC}$), voltage loss due to concentration polarization ($V_{cnc-DAFC}$), and Ohmic loss in voltage ($V_{Ohm-DAFC}$) as follows [18]:

$$V_{OPN-DAFC} = V_{OC-DAFC} + V_{ac-DAFC} + V_{cnc-DAFC} + V_{Ohm-DAFC} \quad (30)$$

where the voltage loss due to Ohmic polarization is evaluated from the operational DAFC current density (I_{D-DAFC}) and DAFC Ohmic resistance (Ω_{DAFC}) as [18]:

$$V_{Ohm-DAFC} = I_{D-DAFC}\Omega_{DAFC} \quad (31)$$

The voltage loss induced in the DAFC due to concentration polarization can be evaluated as a function of the operational temperature (T_{DAFC}), operational current density (I_{D-DAFC}), and limiting current density (I_{L-DAFC}) as [30]:

$$V_{cnc-DAFC} = \frac{RT_{DAFC}}{\alpha Fn} \ln\left(\frac{I_{D-DAFC}}{I_{L-DAFC} - I_{D-DAFC}}\right) \quad (32)$$

The DAFC power output is related to the total current output ($I_{tot-DAFC}$) and operational voltage ($V_{OPN-DAFC}$) as [30]:

$$\dot{P}_{DAFC-out} = V_{OPN-DAFC} I_{tot-DAFC} \quad (33)$$

IV. RESULTS AND DISCUSSION

Simulations of the proposed methodology are conducted using real solar and wind power profiles that have been imported to MATLAB for obtaining the smoothed filter outputs. Engineering Equation Solver (EES) software [46] is used to implement the models for EAS and DAFC systems. The solar PV profile displayed in Fig. 3 was obtained from the University of Queensland-Saint Lucia campus solar live feed database. The fluctuating wind power plot shown in Fig. 12 was acquired from, roaring 40s wind park, Tasmania, Australia. Power smoothing, through the utilization of appropriate filters, is an effective method for reducing the amount of required storage capacity, discharge power requirements, and time delays associated with such energy storage systems.

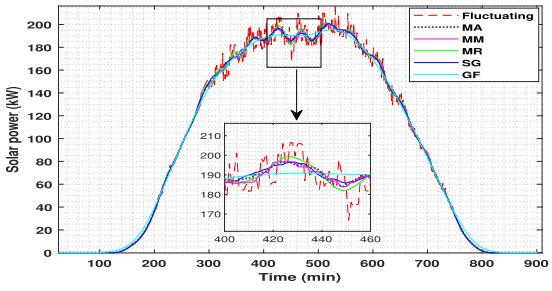

FIGURE 3. Solar power smoothing using the MA, MM, MR, SG, and GF filtration techniques.

The results depicted in Fig. 3 suggest that different types of smoothing filters provide various smoothing levels of

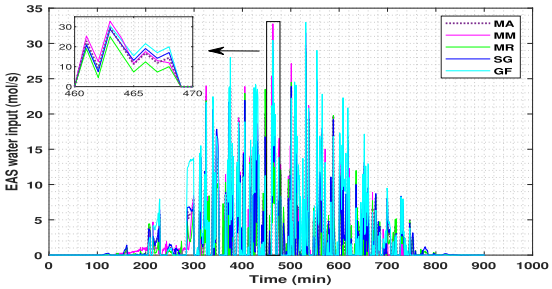

FIGURE 4. EAS water input requirements using the MA, MM, MR, SG, and GF filtration techniques (solar power).

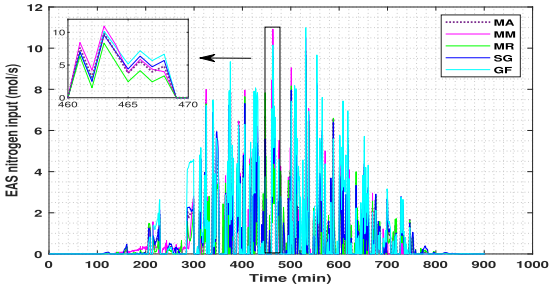

FIGURE 5. EAS nitrogen input requirements using the MA, MM, MR, SG, and GF filtration techniques (solar power).

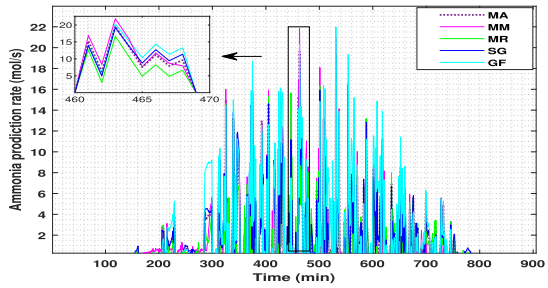

FIGURE 6. EAS ammonia production rates using the MA, MM, MR, SG, and GF filtration techniques (solar power).

solar power output. However, the appropriate filter type can be assessed based on the associated energy storage requirements. The water and nitrogen input requirements, and ammonia production rates of the EAS for electrochemical ammonia synthesis during excess power periods are depicted in Figures 4-6. The results show that the choice of smoothing filter impacts the water and nitrogen input rates as well as the ammonia production rate and the corresponding EAS capacity requirements. Higher ammonia production requirements correspond to higher EAS capacity requirements, which lead to higher overall system costs. Additionally, there is a loss of efficiency with an increase in ammonia production [30].

The DAFC ammonia input rate, depicted in Fig. 7, shows that the MR smoothing filter results in the lowest peak ammonia input requirement for the DAFC of 150 mol/s, while the GF filter has a considerably higher peak ammonia input requirement of nearly 230 mol/s. These are associated with the corresponding ammonia storage costs. Higher ammonia input requirements necessitate higher ammonia storage

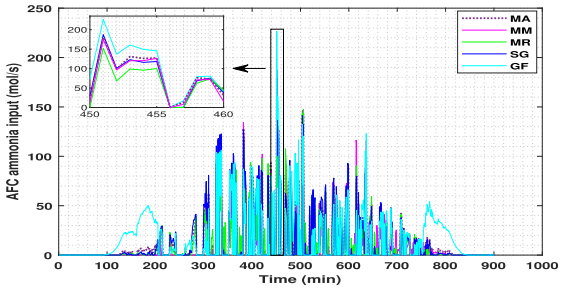

FIGURE 7. DAFC ammonia input rates using the MA, MM, MR, SG, and GF filtration techniques (solar power).

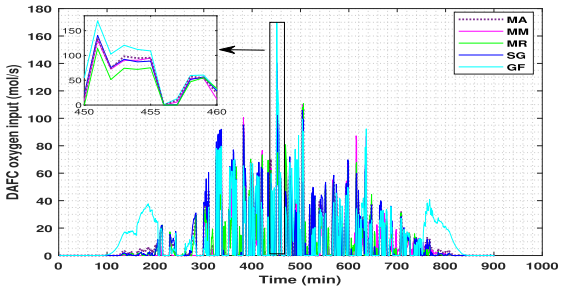

FIGURE 8. DAFC oxygen input rates using the MA, MM, MR, SG, and GF filtration techniques (solar power).

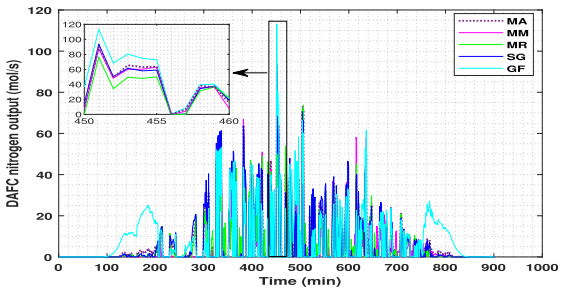

FIGURE 9. DAFC nitrogen output rates using the MA, MM, MR, SG, and GF filtration techniques (solar power).

capacities and thus system costs. Hence, it is recommended to utilize smoothing filters that entail the least ammonia input requirements. Furthermore, the performance of the DAFC plays a key role in determining the ammonia input requirements.

The oxygen input requirements, nitrogen output, and water output from the DAFC are depicted in Figures 8-10. The peak oxygen input requirement reaches nearly 110 mol/s for the MR smoothing filter, while the peak value reaches nearly 170 mol/s for the G filter. Higher oxygen input requirements result in higher oxygen storage costs in the case of the utilization of pure oxygen feed. To reduce this cost, air can be used as the oxidant feed input. The peak water output from the DAFC is observed to reach 225 mol/s for the MR filter, while the peak output of water associated with the G filter entails a value of 340 mol/s.

The power output results obtained for the DAFC utilized during periods of time when the solar energy available is lower than what is required to provide the smoothed power

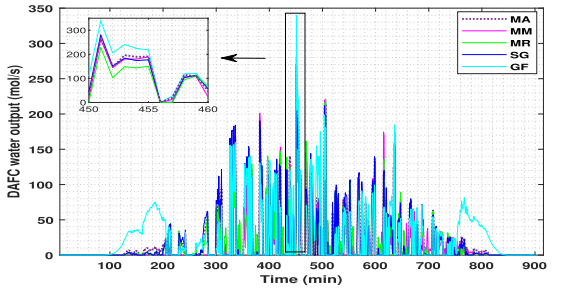

FIGURE 10. DAFC water output rates using the MA, MM, MR, SG, and GF filtration techniques (solar power).

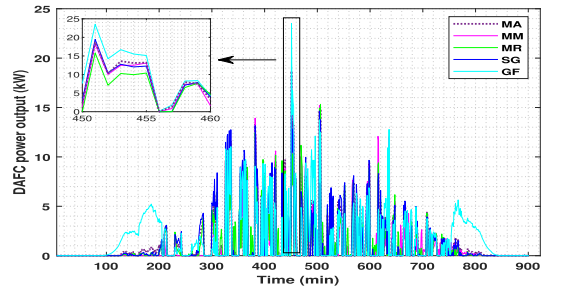

FIGURE 11. DAFC power outputs using the MA, MM, MR, SG, and GF filtration techniques (solar power).

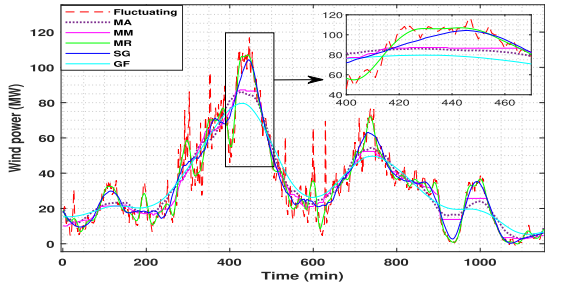

FIGURE 12. Wind power smoothing using the MA, MM, MR, SG, and GF filtration techniques.

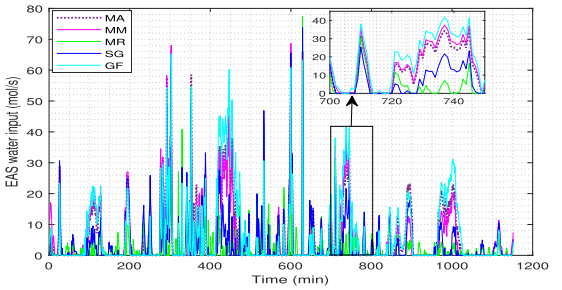

FIGURE 13. EAS water input requirements using the MA, MM, MR, SG, and GF filtration techniques (wind power).

output are depicted in Fig. 11. The results show that the MR smoothing filter provides optimal power smoothing along with minimal peak DAFC power outputs (Fig. 11) as well as minimal peak ammonia production requirements in the EAS (Fig. 6). The MR smoothing filter is found to provide comparatively favorable results under these criteria, and its implementation can lead to reduced system costs, enhanced system efficiencies, and improved grid stability.

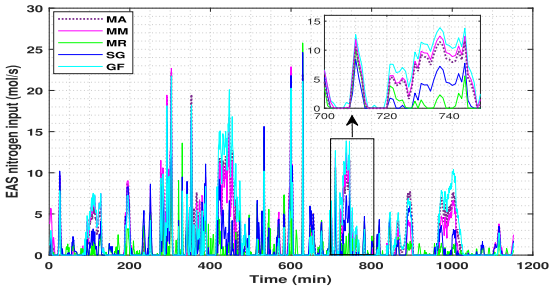

FIGURE 14. EAS nitrogen input requirements using the MA, MM, MR, SG, and GF filtration techniques (wind power).

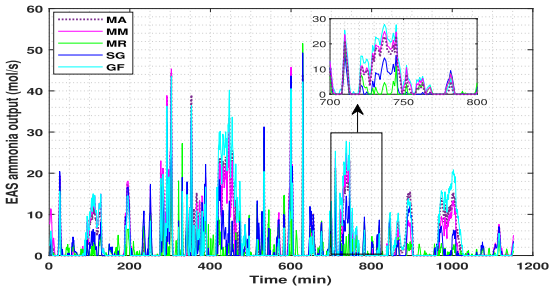

FIGURE 15. EAS ammonia production rates using the MA, MM, MR, SG, and GF filtration techniques (wind power).

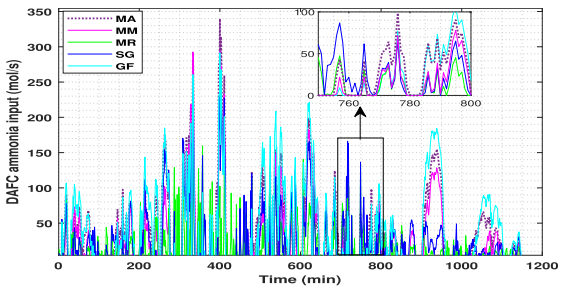

FIGURE 16. DAFC ammonia input rates using the MA, MM, MR, SG, and GF filtration techniques (wind power).

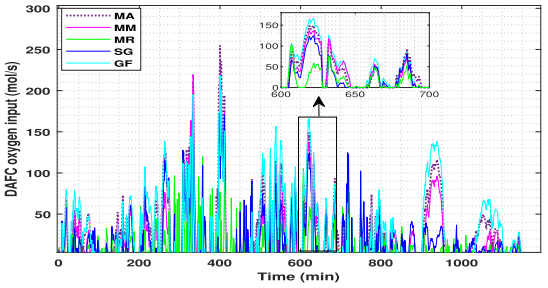

FIGURE 17. DAFC oxygen input rates using the MA, MM, MR, SG, and GF filtration techniques (wind power).

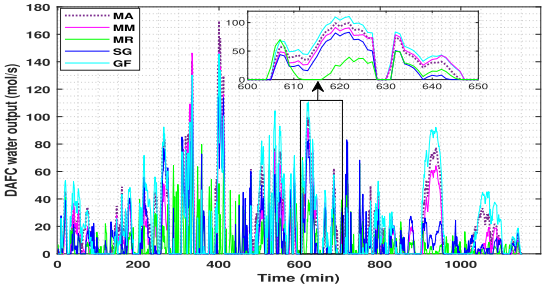

FIGURE 18. DAFC nitrogen output rates using the MA, MM, MR, SG, and GF filtration techniques (wind power).

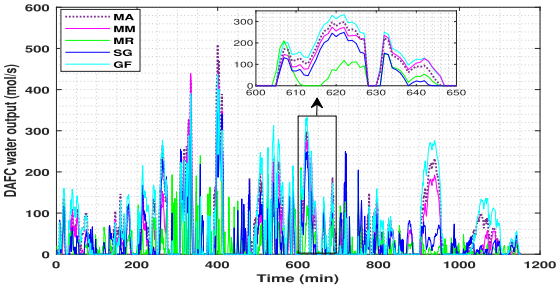

FIGURE 19. DAFC water output rate using the MA, MM, MR, SG, and GF filtration techniques (wind power).

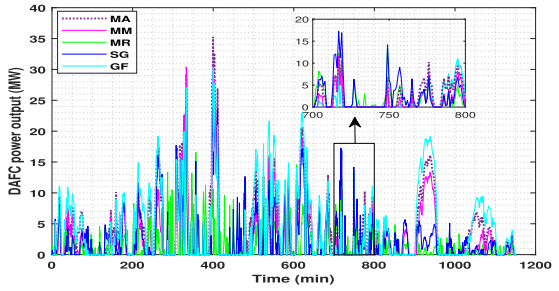

FIGURE 20. DAFC power outputs using the MA, MM, MR, SG, and GF filtration techniques (wind power).

In addition, the use of renewable energy sources such as wind also requires effective power smoothing techniques to ensure a consistent and reliable energy supply. Hence, in this study, different smoothing filters, and their performances in power smoothing for wind-based power generation were also investigated. The results depicted in Fig. 12 indicate that the MR filter is associated with the least time delay as compared with other investigated filters, making it a favorable choice for wind-based power generation. On the other hand, the G filter was found to have the highest power differentials with respect to the original power signal, which may result in instability in the energy supply as well as higher energy storage costs.

Excess power available can also be utilized for electrochemical ammonia synthesis (EAS). The results depicted in Figures 13-15 indicate that the MR filter is associated with the lowest EAS ammonia output capacities as well as associated water and nitrogen input requirements. The SG filter also performed well in this regard. However, the G filter was associated with higher requirements of ammonia production and storage to attain smoothed power outputs. These results highlight the importance of selecting appropriate smoothing filters to optimize EAS capacities and enhance the overall efficiency of the system.

Meeting power deficits with low energy storage requirements is another important consideration in wind-based energy systems. The results depicted in Figures 16-20 indicate that the MR filter is associated with considerably lower requirements of ammonia inputs as well as DAFC power output capacities as compared to the G filter. The MR filter was observed to entail nearly three times lower requirements in terms of EAS capacity, ammonia storage, and

DAFC power output as compared to the G filter. These results suggest that the MR filter may be a more cost-effective option for meeting power deficits in renewable energy systems.

V. CONCLUSION

Ammonia is a sustainable fuel that works well for storing energy from solar and wind power plants. This inspired the current study's investigation into the smoothing and regulation of solar and wind power using ammonia fuel cells. Power output fluctuations can be mitigated with smoothing filters such as the Moving Average, Moving Median, Moving Regression, Savitzky-Golay, and Gaussian. The excess power is used by an electrochemical ammonia synthesizer to generate ammonia. A direct ammonia fuel cell uses the stored ammonia to produce the power deficit, ensuring a smooth and consistent power at the point of connection to the grid. The Moving Regression smoothing filter was identified to provide more effective smoothing to power with lower requirements on ammonia production and storage, and fuel cell power capacities, lowering the overall cost of the system. The proposed technique, which makes use of electrochemical ammonia production and oxidation, has been shown to be an effective method for regulating and smoothing the power produced from solar and wind energy resources.

ACKNOWLEDGMENT

The authors would like to thank the Natural Sciences and Engineering Research Council of Canada (NSERC) for their financial support.

CONFLICT OF INTEREST

The authors declare that there is no known conflict of interest regarding the work reported in this paper.

REFERENCES

[1] H. A. Aalami and S. Nojavan, "Energy storage system and demand response program effects on stochastic energy procurement of large consumers considering renewable generation," *IET Gener., Transmiss. Distribution*, vol. 10, no. 1, pp. 107–114, Jan. 2016.
[2] E. Morgan, J. Manwell, and J. McGowan, "Wind-powered ammonia fuel production for remote islands: A case study," *Renew. Energy*, vol. 72, pp. 51–61, Dec. 2014.
[3] U. T. Salman, F. S. Al-Ismail, and M. Khalid, "Optimal sizing of battery energy storage for grid-connected and isolated wind-penetrated microgrid," *IEEE Access*, vol. 8, pp. 91129–91138, 2020.
[4] M. Khalid and M. A. Syed, "Systems and methods for wind power control and battery size-reduction," U.S. Patent 11 894 683, Feb. 6, 2024.
[5] R. Prasad and N. P. Padhy, "Synergistic frequency regulation control mechanism for DFIG wind turbines with optimal pitch dynamics," *IEEE Trans. Power Syst.*, vol. 35, no. 4, pp. 3181–3191, Jul. 2020.
[6] S. N. Mtolo and A. K. Saha, "A review of the optimization and control strategies for fuel cell power plants in a microgrid environment," *IEEE Access*, vol. 9, pp. 146900–146920, 2021.
[7] Y. Wang, Z. Sun, X. Li, X. Yang, and Z. Chen, "A comparative study of power allocation strategies used in fuel cell and ultracapacitor hybrid systems," *Energy*, vol. 189, Dec. 2019, Art. no. 116142.
[8] S. Alshahrani, M. Khalid, and M. Almuhaini, "Electric vehicles beyond energy storage and modern power networks: Challenges and applications," *IEEE Access*, vol. 7, pp. 99031–99064, 2019.
[9] N. A. El-Taweel, H. Khani, and H. E. Z. Farag, "Hydrogen storage optimal scheduling for fuel supply and capacity-based demand response program under dynamic hydrogen pricing," *IEEE Trans. Smart Grid*, vol. 10, no. 4, pp. 4531–4542, Jul. 2019.
[10] O. Siddiqui and I. Dincer, "Design and analysis of a novel solar-wind based integrated energy system utilizing ammonia for energy storage," *Energy Convers. Manage.*, vol. 195, pp. 866–884, Sep. 2019.
[11] M. A. Syed and M. Kazerani, "Neural network modeling of an electrochemical ammonia synthesizer for smart grid applications," in *Proc. 8th IEEE Workshop Electron. Grid (eGRID)*, Oct. 2023, pp. 1–6.
[12] S. Thaker, A. Olufemi Oni, and A. Kumar, "Techno-economic evaluation of solar-based thermal energy storage systems," *Energy Convers. Manage.*, vol. 153, pp. 423–434, Dec. 2017.
[13] Y. Wang, S. Zheng, J. Chen, Z. Wang, and S. He, "Ammonia (NH3) storage for massive PV electricity," *Energy Procedia*, vol. 150, pp. 99–105, Sep. 2018.
[14] C. Chen, K. M. Lovegrove, A. Sepulveda, and A. S. Lavine, "Design and optimization of an ammonia synthesis system for ammonia-based solar thermochemical energy storage," *Sol. Energy*, vol. 159, pp. 992–1002, Jan. 2018.
[15] M. Al-Zareer, I. Dincer, and M. A. Rosen, "Heat transfer and thermodynamic analyses of a novel solid–gas thermochemical strontium chloride–ammonia thermal energy storage system," *J. Heat Transf.*, vol. 140, no. 2, Feb. 2018.
[16] F. Baldi, A. Azzi, and F. Maréchal, "From renewable energy to ship fuel: Ammonia as an energy vector and mean for energy storage," *Comput. Aided Chem. Eng.*, vol. 46, pp. 1747–1752, 2019.
[17] A. Hasan and I. Dincer, "Development of an integrated wind and PV system for ammonia and power production for a sustainable community," *J. Cleaner Prod.*, vol. 231, pp. 1515–1525, Sep. 2019.
[18] O. Siddiqui and I. Dincer, "A novel hybrid ammonia fuel cell and thermal energy storage system," *Int. J. Energy Res.*, vol. 43, no. 7, pp. 3006–3010, Jun. 2019.
[19] K. H. Rouwenhorst, A. G. Van der Ham, G. Mul, and S. R. Kersten, "Islanded ammonia power systems: Technology review & conceptual process design," *Renew. Sustain. Energy Rev.*, vol. 114, Oct. 2019, Art. no. 109339.
[20] H. Zhang, L. Wang, J. Van Herle, F. Maréchal, and U. Desideri, "Techno-economic comparison of green ammonia production processes," *Appl. Energy*, vol. 259, Feb. 2020, Art. no. 114135.
[21] J. Ikäheimo, J. Kiviluoma, R. Weiss, and H. Holttinen, "Power-to-ammonia in future north European 100 % renewable power and heat system," *Int. J. Hydrogen Energy*, vol. 43, no. 36, pp. 17295–17308, Sep. 2018.
[22] Z. Wan, Y. Tao, J. Shao, Y. Zhang, and H. You, "Ammonia as an effective hydrogen carrier and a clean fuel for solid oxide fuel cells," *Energy Convers. Manage.*, vol. 228, Jan. 2021, Art. no. 113729.
[23] M. A. Syed, O. Siddiqui, M. Kazerani, and M. Khalid, "Analysis of electrochemical ammonia production rate via smoothing filters for solar energy storage," in *Proc. IEEE Can. Conf. Electr. Comput. Eng. (CCECE)*, Sep. 2023, pp. 593–598.
[24] M. B. Abdelghany, M. Faisal Shehzad, D. Liuzza, V. Mariani, and L. Glielmo, "Modeling and optimal control of a hydrogen storage system for wind farm output power smoothing," in *Proc. 59th IEEE Conf. Decis. Control (CDC)*, Dec. 2020, pp. 49–54.
[25] M. A. Syed and M. Khalid, "Machine learning based controlled filtering for solar PV variability reduction with BESS," in *Proc. Int. Conf. Sustain. Energy Future Electric Transp. (SEFET)*, Jan. 2021, pp. 1–5.
[26] V. M. Maestre, A. Ortiz, and I. Ortiz, "Challenges and prospects of renewable hydrogen-based strategies for full decarbonization of stationary power applications," *Renew. Sustain. Energy Rev.*, vol. 152, Dec. 2021, Art. no. 111628.
[27] T. Cai, M. Dong, H. Liu, and S. Nojavan, "Integration of hydrogen storage system and wind generation in power systems under demand response program: A novel p-robust stochastic programming," *Int. J. Hydrogen Energy*, vol. 47, no. 1, pp. 443–458, Jan. 2022.
[28] M. A. Syed and M. Khalid, "An intelligent model predictive control strategy for stable solar-wind renewable power dispatch coupled with hydrogen electrolyzer and battery energy storage," *Int. J. Energy Res.*, vol. 2023, pp. 1–17, Mar. 2023.
[29] A. Iqbal, A. Waqar, R. Madurai Elavarasan, M. Premkumar, T. Ahmed, U. Subramaniam, and S. Mekhilef, "Stability assessment and performance analysis of new controller for power quality conditioning in microgrids," *Int. Trans. Electr. Energy Syst.*, vol. 31, no. 6, Jun. 2021.
[30] I. Dincer and O. Siddiqui, *Ammonia Fuel Cells*. Amsterdam, The Netherlands: Elsevier, 2020.
[31] K. S. Gabriel, R. S. El-Emam, and C. Zamfirescu, "Technoeconomics of large-scale clean hydrogen production—A review," *Int. J. Hydrogen Energy*, vol. 47, no. 72, pp. 30788–30798, Aug. 2022.

[32] M. A. Syed and M. Khalid, "A feedforward neural network hydrogen electrolyzer output regulator for wind power control with battery storage," in *Proc. IEEE PES Innov. Smart Grid Technol. Asia (ISGT Asia)*, Dec. 2021, pp. 1–5.
[33] K. D. Malamaki, F. Casado-Machado, M. Barragán-Villarejo, A. M. Gross, G. C. Kryonidis, J. L. Martinez-Ramos, and C. S. Demoulias, "Ramp-rate limitation control of distributed renewable energy sources via supercapacitors," *IEEE Trans. Ind. Appl.*, vol. 58, no. 6, pp. 7581–7594, Nov. 2022.
[34] M. A. Syed and M. Khalid, "Moving regression filtering with battery state of charge feedback control for solar PV firming and ramp rate curtailment," *IEEE Access*, vol. 9, pp. 13198–13211, 2021.
[35] A. M. Colak and K. Kayisli, "Reducing voltage and frequency fluctuations in power systems using smart power electronics technologies: A review," in *Proc. 9th Int. Conf. Smart Grid (icSmartGrid)*, Jun. 2021, pp. 197–200.
[36] M. A. Syed and M. Khalid, "Locally weighted filtering for photovoltaic power fluctuation control and time delay reduction with battery energy storage," in *Proc. IEEE Madrid PowerTech*, Jun. 2021, pp. 1–5.
[37] R. Kini, D. Raker, T. Stuart, R. Ellingson, M. Heben, and R. Khanna, "Mitigation of PV variability using adaptive moving average control," *IEEE Trans. Sustain. Energy*, vol. 11, no. 4, pp. 2252–2262, Oct. 2020.
[38] L. M. S. de Siqueira and W. Peng, "Control strategy to smooth wind power output using battery energy storage system: A review," *J. Energy Storage*, vol. 35, Mar. 2021, Art. no. 102252.
[39] M. A. Syed and M. Khalid, "Hodrick prescott decomposition for battery energy storage size reduction and wind power control for microgrid applications," in *Proc. IEEE PES Innov. Smart Grid Technol. Conf. - Latin Amer. (ISGT Latin America)*, Sep. 2021, pp. 1–5.
[40] A. Atif and M. Khalid, "Saviztky–Golay filtering for solar power smoothing and ramp rate reduction based on controlled battery energy storage," *IEEE Access*, vol. 8, pp. 33806–33817, 2020.
[41] M. A. Syed and M. Khalid, "Machine learning based hydrogen electrolyzer control strategy for solar power output and battery state of charge regulation," in *Proc. IEEE PES Innov. Smart Grid Technol. Eur. (ISGT Europe)*, Oct. 2021, pp. 1–5.
[42] A. A. Abdalla and M. Khalid, "Smoothing methodologies for photovoltaic power fluctuations," in *Proc. 8th Int. Conf. Renew. Energy Res. Appl. (ICRERA)*, Nov. 2019, pp. 342–346.
[43] M. A. Syed, A. A. Abdalla, A. Al-Hamdi, and M. Khalid, "Double moving average methodology for smoothing of solar power fluctuations with battery energy storage," in *Proc. Int. Conf. Smart Grids Energy Syst. (SGES)*, Nov. 2020, pp. 291–296.
[44] M. A. Syed and M. Khalid, "Neural network predictive control for smoothing of solar power fluctuations with battery energy storage," *J. Energy Storage*, vol. 42, Oct. 2021, Art. no. 103014.
[45] A. Addisu, L. George, P. Courbin, and V. Sciandra, "Smoothing of renewable energy generation using Gaussian-based method with power constraints," *Energy Proc.*, vol. 134, pp. 171–180, Oct. 2017.
[46] K. Klein and F. Alvarado, *EES-Engineering Equation Solver, Version 6.648 ND*. Middleton, WI, USA: FChart Software, 2004.

MISWAR A. SYED (Member, IEEE) was born in Khobar, Saudi Arabia, in 1998. He received the bachelor's degree in electrical engineering from the King Fahd University of Petroleum and Minerals (KFUPM), Dhahran, Saudi Arabia, in 2021. He is currently pursuing the master's degree with the Department of Electrical and Computer Engineering, University of Waterloo, Canada. He has authored/coauthored several journal and conference papers in the field of control and optimization for renewable energy systems. His current research interests include renewable energy resources, distributed power generation, AI-based control and optimization techniques for renewable energy dispatch in grid-connected plants, energy storage, green hydrogen and ammonia, EVs, and machine learning applications in smart grids. He has multiple granted patents. He received multiple awards, including the highly prestigious 2023 IEEE Power & Energy Society Outstanding Student Scholarship.

OSAMAH SIDDIQUI (Member, IEEE) was a Postdoctoral Researcher and a Teaching Fellow with The University of British Columbia. He has authored a book on ammonia fuel cells and more than 30 peer-reviewed journal articles. His research interest includes the development of high-efficiency direct ammonia fuel cells and their integration into renewable energy systems.

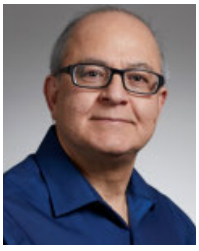

MEHRDAD KAZERANI (Life Senior Member, IEEE) received the B.Sc. degree in electrical engineering from Shiraz University, Iran, in 1980, the master's degree in electrical engineering from Concordia University, Canada, in 1990, and the Ph.D. degree in electrical engineering from McGill University, Canada, in 1995. From 1982 to 1987, he was with the Energy Ministry of Iran. He is currently a Professor with the Department of Electrical and Computer Engineering, University of Waterloo, Waterloo, ON, Canada. His research interests include energy storage, battery charging systems, transportation electrification, renewable energy integration, microgrids, current-sourced converter applications, and matrix converters. He is a Registered Professional Engineer in the Province of Ontario.

MUHAMMAD KHALID (Senior Member, IEEE) received the Ph.D. degree in electrical engineering from the School of Electrical Engineering Telecommunications (EET), The University of New South Wales (UNSW), Sydney, Australia, in 2011. He was initially a Postdoctoral Research Fellow, for three years, and then he continued as a Senior Research Associate with Australian Energy Research Institute, School of EET, UNSW, for two years. He is currently an Associate Professor with the Electrical Engineering Department, King Fahd University of Petroleum and Minerals (KFUPM), Dhahran, Saudi Arabia. He is also a Research Affiliate with the Interdisciplinary Research Center for Sustainable Energy Systems, KFUPM. He has authored/coauthored several journals and conference papers in the field of control and optimization for renewable power systems. His research interests include the optimization and control of battery energy storage systems for large-scale grid-connected renewable power plants (particularly wind and solar), distributed power generation and dispatch, hybrid energy storage, hydrogen systems, EVs, AI, machine learning, and smart grids. He was a recipient of the Highly Competitive Postdoctoral Writing Fellowship from UNSW, in 2010. He was a recipient of many academic awards and research fellowships. In addition, he has been a reviewer of numerous international journals and conferences.